H7N9 Influenza Viruses Are Transmissible in Ferrets by Respiratory Droplet

Qianyi Zhang *et al.*

Science **341**, 410 (2013);
DOI: 10.1126/science.1240532

Science (print ISSN 0036-8075; online ISSN 1095-9203) is published weekly, except the last week in December, by the American Association for the Advancement of Science, 1200 New York Avenue NW, Washington, DC 20005.

enzymes involved in glucose and cholesterol metabolism between the various intestinal segments of RYGB-treated rats and corresponding segments of the intestine of sham-operated rats. A gradient in the change in RNA levels of key factors and enzymes involved in glucose uptake and utilization and in cholesterol biosynthesis and uptake was observed along the altered nutrient flow path in the intestine of RYGB-treated rats (figs. S11 and S12). The highest increase was detected in the Roux limb, which is exposed to undigested nutrients, but no change was found in the biliopancreatic limb, which is exposed to the gastric, hepatic, and pancreatic secretions but no nutrients, or in the distal common limb, which is exposed to fully digested nutrients.

The effectiveness of RYGB in the resolution of type 2 diabetes attests to the important role of the gastrointestinal tract in glycemic control. Most studies have attributed the improved glucose metabolism to a number of advantageous changes in the levels of gastrointestinal hormones that control glucose homeostasis and occur after RYGB, with enhanced postprandial glucagon-like peptide-1 (GLP-1) secretion being cited as the most important (*3*, *8*, *24*). However, the primary role of GLP-1 as a mediator of the beneficial effect of RYGB on glycemic control is debated (*25*, *26*). It has also been reported that release of glucose, via intestinal gluconeogenesis, into the portal vein of mice that underwent enterogastric anastomosis (EGA), resulted in improved insulin sensitivity of hepatic glucose production; thus, it has been hypothesized that intestinal gluconeogenesis could account for the improvement in glucose homeostasis after RYGB (*27*). It should be noted that EGA is not similar to RYGB, because the Roux-en-Y configuration is not constructed and no intestinal segment is representative of the Roux limb. Also, two recent reports in obese diabetic animals and in humans with type 2 diabetes and our study did not find evidence for induction of intestinal gluconeogenesis after RYGB (*28*, *29*). A decrease in intestinal glucose absorptive capacity due to the exclusion of the duodenum after RYGB has also been proposed as a mechanism underlying the improvement in glycemic control (*11*), but other studies have found that RYGB does not suppress glucose absorption from the intestinal lumen (*10*, *30*–*32*).

Our study shows that changes in the metabolism of the Roux limb itself may play a direct role in the improvement in glucose homeostasis after RYGB. We report that the Roux limb exhibits reprogramming of intestinal glucose metabolism to meet the increased bioenergetic demands of intestinal remodeling. We show that intestinal remodeling and reprogramming of intestinal glucose metabolism are triggered by the exposure of the Roux limb to undigested nutrients. We demonstrate that reprogramming of intestinal glucose metabolism renders the intestine a major organ for glucose disposal, contributing to the improvement in glycemic control after RYGB. Enhancing intestinal glucose uptake and utilization could offer an opportunity to regulate whole-body glucose disposal and improve glycemic control in type 2 diabetes. Exploitation of the changes that occur in intestinal metabolism after RYGB could represent an approach to bypass the bypass, that is, to replace the gastric bypass by equally effective, but less invasive, treatments for obesity-related diabetes.

References and Notes

1. H. Buchwald *et al*., *JAMA* **292**, 1724–1737 (2004).
2. L. Sjöström *et al*. Swedish Obese Subjects Study Scientific Group, *N. Engl. J. Med.* **351**, 2683–2693 (2004).
3. M. A. Stefater, H. E. Wilson-Pérez, A. P. Chambers, D. A. Sandoval, R. J. Seeley, *Endocr. Rev.* **33**, 595–622 (2012).
4. G. Mingrone *et al*., *N. Engl. J. Med.* **366**, 1577–1585 (2012).
5. P. R. Schauer *et al*., *N. Engl. J. Med.* **366**, 1567–1576 (2012).
6. L. M. Carlsson *et al*., *N. Engl. J. Med.* **367**, 695–704 (2012).
7. W. J. Pories *et al*., *Ann. Surg.* **222**, 339–352 (1995).
8. B. Laferrère, *Endocrine* **40**, 162–167 (2011).
9. D. E. Cummings, *Nat. Med.* **18**, 656–658 (2012).
10. D. Bradley *et al*., *J. Clin. Invest.* **122**, 4667–4674 (2012).
11. A. T. Stearns, A. Balakrishnan, A. Tavakkolizadeh, *Am. J. Physiol. Gastrointest. Liver Physiol.* **297**, G950–G957 (2009).
12. M. B. Mumphrey, L. M. Patterson, H. Zheng, H. R. Berthoud, *Neurogastroenterol. Motil.* **25**, e70–e79 (2013).
13. E. Spak *et al*., *Histopathology* **57**, 680–688 (2010).
14. E. Taqi *et al*., *J. Pediatr. Surg.* **45**, 987–995 (2010).
15. C. W. le Roux *et al*., *Ann. Surg.* **252**, 50–56 (2010).
16. M. Bueter *et al*., *Gastroenterology* **138**, 1845–1853, 1853.e1 (2010).
17. J. Kucharczyk, E. Nestoridi, S. Kvas, R. Andrews, N. Stylopoulos, *J. Surg. Res.* **179**, e91–e98 (2013).
18. E. Nestoridi, S. Kvas, J. Kucharczyk, N. Stylopoulos, *Endocrinology* **153**, 2234–2244 (2012).
19. Materials and methods are available as supplementary materials on *Science* Online.
20. S. Y. Lunt, M. G. Vander Heiden, *Annu. Rev. Cell Dev. Biol.* **27**, 441–464 (2011).
21. M. G. Vander Heiden, L. C. Cantley, C. B. Thompson, *Science* **324**, 1029–1033 (2009).
22. B. Thorens, *Am. J. Physiol.* **270**, G541–G553 (1996).
23. J. Pácha, *Physiol. Rev.* **80**, 1633–1667 (2000).
24. Y. Falkén, P. M. Hellström, J. J. Holst, E. Näslund, *J. Clin. Endocrinol. Metab.* **96**, 2227–2235 (2011).
25. J. M. Isbell *et al*., *Diabetes Care* **33**, 1438–1442 (2010).
26. H. E. Wilson-Pérez *et al*., *Diabetes* **62**, 2380–2385 (2013).
27. S. Troy *et al*., *Cell Metab.* **8**, 201–211 (2008).
28. B. S. Wolff, K. Meirelles, Q. Meng, M. Pan, R. N. Cooney, *Am. J. Physiol. Gastrointest. Liver Physiol.* **297**, G594–G601 (2009).
29. M. T. Hayes, J. Foo, V. Besic, Y. Tychinskaya, R. S. Stubbs, *Obes. Surg.* **21**, 759–762 (2011).
30. F. Rubino *et al*., *Ann. Surg.* **244**, 741–749 (2006).
31. F. Rodieux, V. Giusti, D. A. D'Alessio, M. Suter, L. Tappy, *Obesity (Silver Spring)* **16**, 298–305 (2008).
32. G. Wang *et al*., *Obes. Surg.* **22**, 1263–1267 (2012).

Acknowledgments: We thank N. Li for help with tissue sectioning, G. Gorski for help with electron microscopy, M. Markle and M. Luitje for help with biodistribution analysis, and A. Moses for help with lipid analysis. This research was supported by funds from the Department of Medicine and the Clinical and Translational Executive Committee at Boston Children's Hospital (N. Stylopoulos) and grants T32DK007191 (N.K.G.) and F32DK095558 (N. Saeidi) from the National Institutes of Health (NIH). We used the core services of the Lipidomics Lab at the Nutrition Obesity Research Center of the University of Michigan (Ann Arbor, MI), which is supported by grant DK089503 from NIH.

Supplementary Materials

www.sciencemag.org/cgi/content/full/341/6144/406/DC1
Materials and Methods
Supplementary Text 1 and 2
Figs. S1 to S12
Table S1
Movies S1 and S2
References (*33*–*37*)

14 January 2013; accepted 13 June 2013
10.1126/science.1235103

H7N9 Influenza Viruses Are Transmissible in Ferrets by Respiratory Droplet

Qianyi Zhang,[1,2]* Jianzhong Shi,[1]* Guohua Deng,[1]* Jing Guo,[1]* Xianying Zeng,[1]* Xijun He,[1] Huihui Kong,[1] Chunyang Gu,[1,2] Xuyong Li,[1] Jinxiong Liu,[1] Guojun Wang,[1,2] Yan Chen,[1] Liling Liu,[1] Libin Liang,[1] Yuanyuan Li,[1] Jun Fan,[1] Jinliang Wang,[1] Wenhui Li,[1] Lizheng Guan,[1] Qimeng Li,[1,2] Huanliang Yang,[1] Pucheng Chen,[1] Li Jiang,[1] Yuntao Guan,[1] Xiaoguang Xin,[1] Yongping Jiang,[1] Guobin Tian,[1] Xiurong Wang,[1] Chuanling Qiao,[1] Chengjun Li,[1] Zhigao Bu,[1] Hualan Chen[1,2]†

A newly emerged H7N9 virus has caused 132 human infections with 37 deaths in China since 18 February 2013. Control measures in H7N9 virus–positive live poultry markets have reduced the number of infections; however, the character of the virus, including its pandemic potential, remains largely unknown. We systematically analyzed H7N9 viruses isolated from birds and humans. The viruses were genetically closely related and bound to human airway receptors; some also maintained the ability to bind to avian airway receptors. The viruses isolated from birds were nonpathogenic in chickens, ducks, and mice; however, the viruses isolated from humans caused up to 30% body weight loss in mice. Most importantly, one virus isolated from humans was highly transmissible in ferrets by respiratory droplet. Our findings indicate nothing to reduce the concern that these viruses can transmit between humans.

The influenza A virus genome comprises eight genes: *basic polymerase 2* (*PB2*), *basic polymerase 1* (*PB1*), *acidic polymerase* (*PA*), *hemagglutinin* (*HA*), *nucleoprotein* (*NP*), *neuraminidase* (*NA*), *matrix* (*M*), and *nonstructural protein* (*NS*). On the basis of differences in the antigenicity of the two surface glycoproteins, HA and NA, influenza A viruses are categorized into

different subtypes. Currently, 17 HA subtypes and 10 NA subtypes have been identified. All subtypes were identified initially from avian species, except for the H17N10 subtype, which was found in bats (*1*).

Animal influenza viruses continue to present a challenge to human health. On 31 March 2013, the National Health and Family Planning Commission of China announced that human infections with a previously undescribed influenza A (H7N9) virus had occurred in Shanghai and Anhui province, China. Additional infections were subsequently reported in seven other provinces. As of 30 May, 132 human infections have been identified, 37 of which were fatal (*2*). Because the H7N9 virus has not previously been detected in humans or other animals, the situation raises many urgent questions and global public health concerns. We performed active surveillance in animals to identify the source of human infection and evaluated the virulence and transmission potential of H7N9 viruses isolated from birds and humans in poultry and mammalian models.

To investigate the possible origins of the H7N9 viruses that caused these human infections, we collected 10,703 samples from poultry markets, poultry farms, wild bird habitats, and poultry and swine slaughterhouses in Shanghai and in Anhui, Zhejiang, Jiangsu, Shandong, Hubei, Henan, Jiangxi, Guangdong, Fujian, and Hunan provinces from 30 March to 2 May 2013 (*3*). All samples were inoculated individually into 10-day-old embryonated chicken eggs for virus isolation; 136 Newcastle disease viruses and 238 influenza viruses were isolated from these samples, of which 52 viruses were confirmed as the H7N9 subtype (table S1). Except for one virus isolated from a homing pigeon farm and one virus isolated from a wild pigeon, all of the H7N9 viruses were isolated from samples collected from live poultry markets (*4*) (table S1).

To understand the genetic relationship of these viruses, we fully sequenced the genome of 37 representative H7N9 viruses that came from different bird species, markets, and locations in the markets for the environmental samples (table S1) and compared the sequences with those of the five human isolates that have been reported (*5*, *6*). The genome similarities of the 37 avian viruses and four human viruses were compared with the human isolate A/Anhui/1/2013 (AH/1) as shown in table S2. The *HA* genes and *NA* genes of these 41 H7N9 viruses shared 99.29 to 100% homology and 99.36 to 99.93% homology, respectively, with those of the AH/1 virus at the nucleotide level and were closely clustered in the phylogenetic tree (table S2 and fig. S1, A and B). The *PB2*, *PB1*, *PA*, *NP*, *M*, and *NS* genes of the 41 viruses shared 96.67 to 99.96%, 96.79 to 99.96%, 97.95 to 99.95%, 97.66 to 100%, 97.66 to 100%, and 97.61 to 100% homology, respectively, at the nucleotide level, with those of AH/1 virus, indicating that the internal genes of the H7N9 viruses are more diverse than their *HA* and *NA* genes and that the viruses are still subject to frequent reassortment and rapid evolution. Of note, in the phylogenetic trees, the six internal genes of the H7N9 viruses were mixed with those of the H9N2 viruses that were previously found in chickens in Shanghai, Zhejing, Jiangsu, Anhui, and Shandong provinces and in a brambling in Beijing (fig. S1, C to H).

Two amino acids in PB2, lysine at position 627 (627K) (*7*) and 701N, are important for influenza virulence and transmission in mammals (*8*–*11*). A detailed comparison of the amino acid differences among the H7N9 viruses indicated that all of the viruses isolated from birds or the environment had the amino acid combination 627E/701D in their PB2; however, all of the

[1]State Key Laboratory of Veterinary Biotechnology, Harbin Veterinary Research Institute, Chinese Academy of Agricultural Sciences, Harbin 150001, People's Republic of China. [2]College of Veterinary Medicine, Gansu Agricultural University, Lanzhou 730030, People's Republic of China.

*These authors contributed equally to this work.
†Corresponding author. E-mail: chenhualan@caas.cn

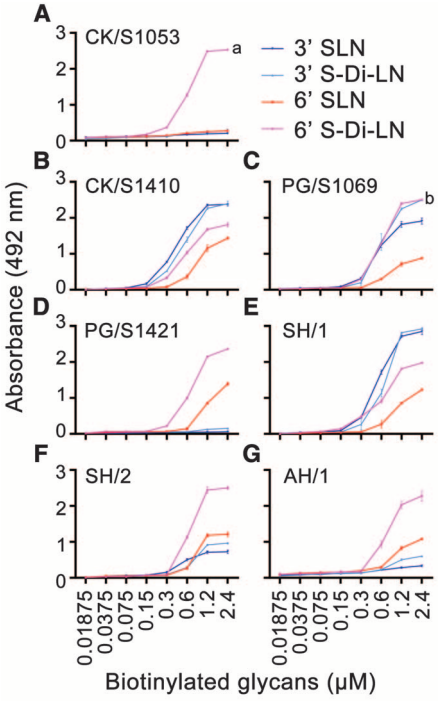

Fig. 1. Characterization of the receptor-binding properties of H7N9 viruses. The binding of the viruses to four different biotinylated glycans (two α-2,3 glycans, blue and Cambridge blue; two α-2,6 glycans, red and pink) was tested. (**A**) CK/S1053; (**B**) CK/S1410; (**C**) PG/S1069; (**D**) PG/S1421; (**E**) SH/1; (**F**) SH/2; (**G**) AH/1. Data shown are the mean of three repeats; the error bars indicate the standard deviations. Significant differences were detected between the affinity of each two of the four glycans with two exceptions: (i) no significant difference was detected between the affinities to 3′SLN and 3′S-Di-LN of the CK/S1053 virus (a), and (ii) no significant difference was detected between the affinities to 3′S-Di-LN and 6′S-Di-LN of PG/S1069 virus (b).

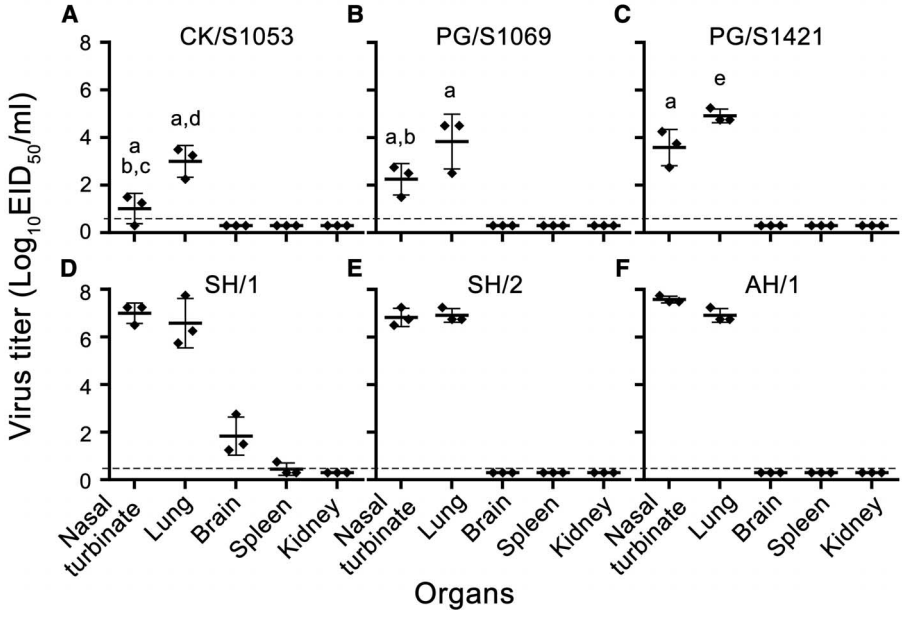

Fig. 2. Replication of H7N9 viruses in mice. Virus titers in organs of mice on day 3 p.i. with 10^6 EID_{50} of the test virus. (**A**) CK/S1053; (**B**) PG/S1069; (**C**) PG/S1421; (**D**) SH/1; (**E**) SH/2; (**F**) AH/1. The data shown are the mean ± standard deviation for each group. a, $P < 0.01$ compared with the corresponding value for the SH/1-, SH/2-, or AH/1-inoculated group; b, $P < 0.01$ compared with the corresponding value for the PG/S1421-inoculated group; c, $P < 0.05$ compared with the corresponding value for the PG/S1069-inoculated group; d, $P < 0.05$ compared with the corresponding value for the PG/S1421-inoculated group; e, $P < 0.05$ compared with the corresponding value for the SH/1-, SH/2-, or AH/1-inoculated group. The dashed lines indicate the lower limit of detection.

human isolates had either 627K or 701N in their PB2 (table S3), suggesting that the PB2 627K or 701N mutations may have occurred during replication of the virus in humans.

The receptor-binding preference of HA has important implications for influenza virus replication and transmission (*12*–*16*). The HA of human-infective influenza subtypes preferentially recognizes α-2,6-linked sialic acids (SAs) (humanlike receptors), whereas the HA of avian-infective influenza subtypes preferentially recognizes α-2,3-linked SAs (avian-like receptors) (*15*, *17*). Mutations at 158D or 160A (H3 numbering used throughout), which result in the absence of glycosylation at position 158 to 160 in HA, combined with mutations at 224K and 226L or at 226L and 228S are important for H5N1 avian influenza virus binding to α-2,6-linked SAs (*10*, *14*). All 42 of the H7N9 viruses isolated from poultry markets and humans had conserved 160A, 224N, and 228G in their HA; 36 isolates had 226L, one had 226I, and the remaining six had 226Q. The amino acid I at position 243 in HA was detected in six isolates, whereas the other 36 viruses had V at 243 in HA (table S3). We, therefore, tested the receptor specificity of seven H7N9 viruses by using a solid-phase binding assay with four different glycans [two α-2,6 glycans: Neu5Acα2-6Galβ1-4GlcNAcβ-SpNH-LC-LC-Biotin (6′SLN) and Neu5Acα2-6[Galβ1-4GlcNAcβ1-3]$_2$β-SpNH-LC-LC-Biotin (6′S-Di-LN); two α-2,3 glycans: Neu5Acα2-3Galβ1-4GlcNAcβ-SpNH-LC-LC-Biotin (3′SLN) and Neu5Acα2-3[Galβ1-4GlcNAcβ1-3]$_2$β-SpNH-LC-LC-Biotin (3′S-Di-LN)] as described previously (*18*): four isolated from birds, A/chicken/Shanghai/S1053/2013 (CK/S1053), A/pigeon/Shanghai/S1069/2013 (PG/S1069) (containing HA 243I), A/chicken/Shanghai/S1410/2013 (CK/S1410) (containing HA 226Q), and A/pigeon/Shanghai/S1421/2013 (PG/S1421), and three isolated from humans, A/Shanghai/1/2013 (SH/1) (containing HA 226Q), A/Shanghai/2/2013 (SH/2), and AH/1. CK/S1053, PG/S1421, SH/2, and AH/1 (Fig. 1, A, D, F, and G) have the same HA, and all four viruses bound to α-2,6-linked SA, 6′S-Di-LN, with high affinity and to α-2,3-linked SAs with very low affinity. However, their affinity for α-2,6-linked SA, 6′SLN, was variable. The factors that contributed to this variability remain unknown. CK/S1410 and SH/1 bound to both α-2,3-linked and α-2,6-linked SAs, with significantly higher affinity for α-2,3-linked SAs than for α-2,6-linked SAs (Fig. 1, B and E). PG/S1069 bound to both α-2,3-linked and α-2,6-linked SAs, and its affinity for the glycans 6′S-Di-LN and 3′S-Di-LN was similar (Fig. 1C). The I to V change at 243 (I243V) is the only amino acid difference in HA between PG/S1069 and AH/1, SH/2, or CK/S1053, and the Q to L change at 226 (Q226L) is the only amino acid difference in HA between CK/S1410 and AH/1, SH/2, or CK/S1053. We therefore speculated that, similar to the Q226L mutation in HA, the I243V mutation may play an important role in the exclusive binding of CK/S1053, PG/S1421, AH/1, and SH/2 to α-2,6-linked SAs.

All H7N9 viruses have a single basic amino acid in their *HA* genes, a characteristic of low pathogenic influenza virus in chickens (*4*, *6*, *19*). To confirm their virulence, we selected two early isolates, one chicken virus (CK/S1053) and one pigeon virus (PG/S1069), which have different receptor binding properties, and tested their intravenous pathogenicity index (IVPI) in chickens (*20*). Groups of 10 6-week-old specific-pathogen-free (SPF) chickens were inoculated intravenously with 0.1 ml of a 1:10 dilution of bacteria-free allantoic fluid containing CK/S1053 or PG/S1069. None of the chickens showed signs of disease or died during the 10-day observation, yielding an IVPI value of 0 (with 3.0 being the most pathogenic and 0 being the least pathogenic), indicating that these H7N9 viruses are nonpathogenic in chickens (table S4).

Infection experiments (*3*) indicated that chickens are easily infected by H7N9 viruses and efficiently shed virus for up to 7 days, suggesting that these birds may be one of the major carriers and spreaders of H7N9 viruses in the live poultry markets.

H7N9 virus infection of humans has caused a 21% mortality rate among hospitalized cases (*21*); however, the wide clinical spectrum of these infections in humans, from mild infection to death, prompted us to investigate the virulence of these viruses in mammals. Mice have been widely used to evaluate the virulence of influenza viruses, and correlations of virulence in mice and in humans have been observed with H5N1 viruses (*22*, *23*).

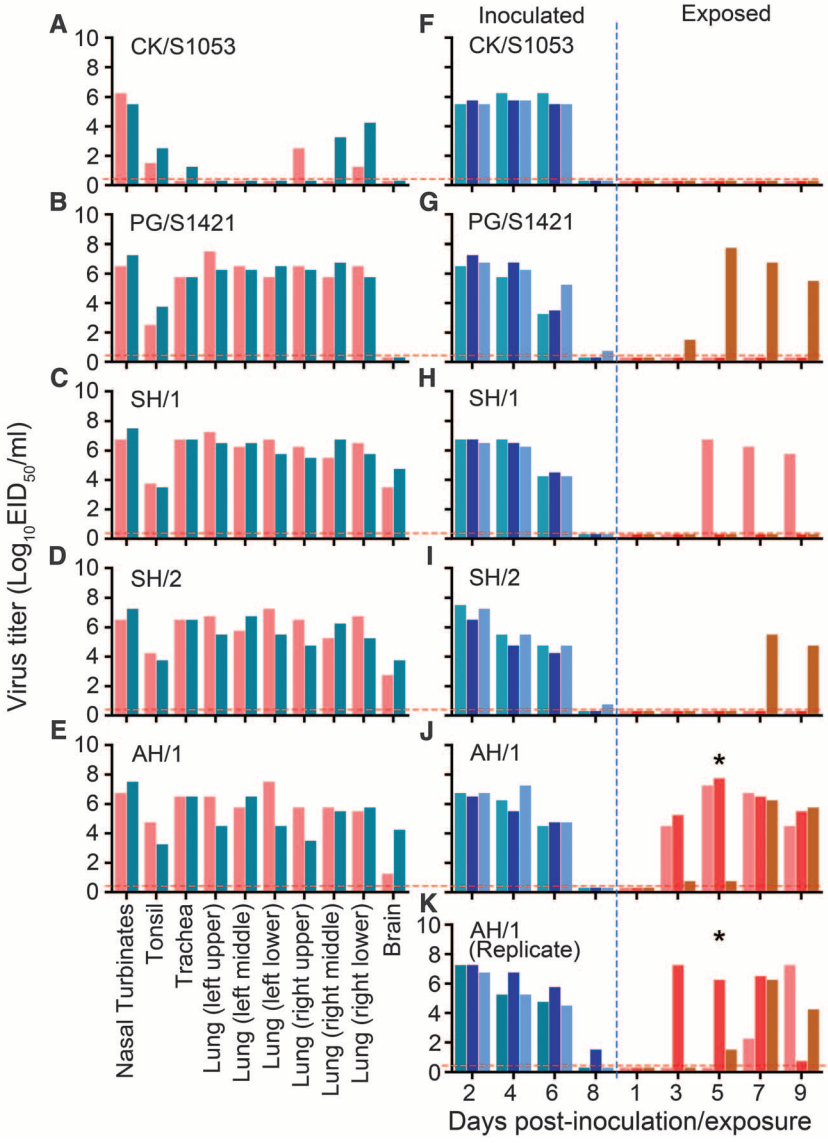

Fig. 3. Replication and respiratory droplet transmission in ferrets of H7N9 viruses. Virus replication: (**A**) CK/S1053; (**B**) PG/S1421; (**C**) SH/1; (**D**) SH/2; (**E**) AH/1. Virus respiratory droplet transmission: (**F**) CK/S1053; (**G**) PG/S1421; (**H**) SH/1; (**I**) SH/2; (**J**) AH/1; (**K**) AH/1 (replicate). Each color bar represents the virus titer from an individual animal. The dashed red lines indicate the lower limit of detection. Asterisks indicate that transmission efficacy was significantly higher than that of the CK/S1053 virus.

We therefore used BALB/c mice to evaluate the replication and virulence of six of the H7N9 viruses: three isolated from poultry, CK/S1053, PG/S1069, and PG/S1421, and three isolated from humans, SH/1, SH/2, and AH/1 (*5*). PG/S1421 and AH/1 are similar in their genome and only differ by a single amino acid at position 627 in their PB2 (table S3).

Mouse lethal dose (MLD_{50}) values were determined by intranasally (i.n.) inoculating groups of five mice with $10^{1.0}$ to $10^{6.0}$ 50% egg infectious dose (EID_{50}) of the virus, and body weight, disease signs, and death were monitored daily for 2 weeks. No disease signs or deaths were observed among mice inoculated with the three viruses isolated from birds, and all mice gained body weight during the observation period (fig. S2, A to C and G to I); in contrast, mice infected with high doses (>10^4 EID_{50}) of the three human isolates experienced weight loss (fig.S2, D to F), and the mice inoculated with 10^6 EID_{50} of SH/1 were killed because they became very sick and lost over 30% of their body weight on day 7 postinfection (p.i.). SH/1 was lethal for mice with an MLD_{50} of 5.4 logEID_{50}, and one mouse in each of the 10^5 and 10^6 EID_{50} of AH/1-inoculated groups and the 10^6 EID_{50} of SH/2-inoculated group died (fig. S2, J to L).

To evaluate the replication of the viruses in mammals, we inoculated groups of three mice i.n. with 10^6 EID_{50} of virus. Mice were killed on day 3 p.i., and their organs, including nasal turbinates, lungs, spleen, kidneys, and brain, were collected for virus titration. Replication of CK/S1053, PG/S1069, PG/S1421, SH/2, and AH/1 was detected in the nasal turbinates and lungs of mice but not in their spleens, kidneys, or brains (Fig. 2, A to C, E, and F); however, SH/1 was detected in the turbinates, lungs, and brains of all three mice and also in the spleen of one mouse (Fig. 2D). Viral titers in the nasal turbinates and lungs of the three human isolate–inoculated mice were significantly

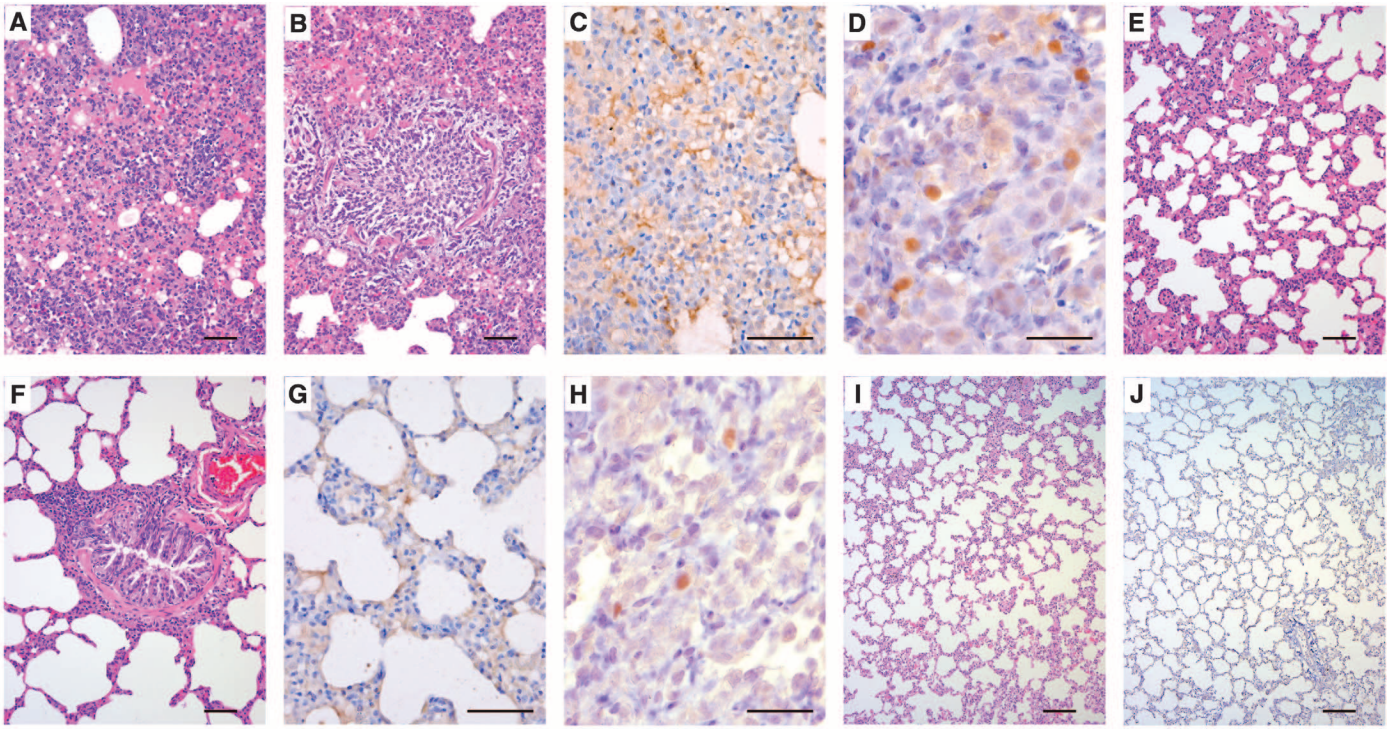

Fig. 4. Histological lesions caused by H7N9 viruses in the lungs of ferrets. Ferrets were killed on day 4 p.i. with 10^6 EID_{50} of the test virus, and the lungs were collected for pathological study. The lungs from the AH/1 virus-infected ferrets developed prominent features of bronchointerstitial pneumonia with massive recruitment of lymphocytes into the lumen and surrounding alveoli and peribronchus, as well as sloughing and necrosis of the respiratory epithelium in the peribronchiolar lumen and submucosal edema of the bronchiolar wall [hematoxylin and eosin (H&E) staining] (**A** and **B**). Viral antigen of AH/1 virus was detected in the epithelial cells of alveoli by means of immunohistochemical (IHC) staining (**C** and **D**). The lungs of a CK/S1053 virus–inoculated animal showed only mild histopathological changes (H&E staining) (**E** and **F**). Limited viral antigen was detected in the lung tissues from CK/S1053 virus–inoculated animals (IHC staining) (**G** and **H**). Normal lung tissues from PBS-inoculated animals [H&E staining (**I**); IHC staining (**J**)]. Scale bars in (A), (C), and (E) to (G), 50 μm; in (D) and (H), 30 μm; in (I) and (J), 100 μm.

Table 1. Virulence and transmission of H7N9 viruses in ferrets. Data shown are from the animal in that group with the maximum body-temperature increase or maximum body-weight loss. Seroconversion was confirmed from the sera of ferrets collected on day 14 (the repeat AH/1 experiment) or on day 21 p.i. The AH/1 transmission experiment was conducted twice; the combined data are presented.

Virus	Maximum body temperature increase (°C)		Maximum body weight loss (%)		Seroconversion (HI antibody titer range)		Respiratory droplet transmission
	Inoculated	Exposed	Inoculated	Exposed	Inoculated	Exposed	
CK/S1053	1.5	0.5	2	1.1	3/3 (160–320)	0/3	None
PG/S1421	2	1.0	7.6	5.8	3/3 (160–320)	1/3 (160)	Lowly efficient
SH/1	1.5	1.3	3.1	2.1	3/3 (160–320)	1/3 (160)	Lowly efficient
SH/2	2.3	1.8	3.5	2.8	3/3 (160–320)	1/3 (80)	Lowly efficient
AH/1	1.7	1.4	3.7	3.1	6/6 (160–640)	6/6 (80–320)	Highly efficient

higher than those in the three bird isolate–inoculated mice (Fig. 2). These results indicate that the H7N9 human isolates replicated much more efficiently and were more lethal in mice than were the viruses isolated from birds and that the PB2 627K mutation likely contributed to the increased virulence of the human isolates to mice, as was observed with H5N1 viruses (*11*).

The H7N9 viruses have caused in excess of 100 human cases in a relatively short period, and the biggest concern around the world is whether these viruses can transmit efficiently from human to human. If these viruses acquire the ability to efficiently transmit among humans, there is a high chance of an influenza pandemic, because humans have no immunity to H7N9 viruses. Therefore, evaluation of the transmissibility of these viruses is important.

Ferrets and guinea pigs have been widely used as animal models for influenza virus transmission studies (*10*, *14*, *15*, *24*, *25*), and human influenza viruses transmit similarly in these two models (*24*, *26*). Transmission studies of influenza mutants with changes in their HA indicate that respiratory droplet transmission appears to be restricted in ferrets if the virus does not exclusively or preferentially bind to α-2,6-linked SA (*24*, *27*); the same may be true for humans, because all widely circulating human influenza viruses preferentially bind to α-2,6-linked SA (*15*, *17*). We therefore tested the replication and respiratory droplet transmission of two avian H7N9 viruses, CK/S1053 and PG/S1421, that preferentially bind to α-2,6-linked SAs and that of the three human H7N9 viruses, SH/1, SH/2, and AH/1, in ferrets.

Two ferrets were inoculated i.n. with 10^6 EID_{50} of each virus, and the nasal turbinates, tonsils, trachea, lungs, spleen, kidneys, brain, and liver from each ferret were collected on day 4 p.i. for virus titration in eggs. The five viruses replicated to similar levels in the nasal turbinates, but the viral titers in the tonsils, trachea, and lungs of ferrets inoculated with CK/S1053 were notably lower than those in ferrets inoculated with PG/S1421 or the three human isolates (Fig. 3, A to E). Virus was also detected in the brains of the ferrets inoculated with the three human isolates but was not detected in the spleen, kidney, or liver of any ferret (Fig. 3, A to E).

Pathological studies were performed on lung samples from the virus-infected ferrets. The lungs of PG/S1421-, SH/1-, SH/2-, and AH/1-infected ferrets showed severe bronchopneumonia with prominent viral antigen expression (Fig. 4, A to D, and fig. S3). By contrast, most of the lung appeared normal after infection with CK/S1053 (Fig. 4, E to H).

To investigate respiratory droplet transmission, we inoculated three ferrets i.n. with 10^6 EID_{50} of test virus and then housed them separately in solid stainless-steel cages within an isolator (fig. S4). Twenty-four hours later, three naïve ferrets were placed in adjacent cages. Each pair of animals was separated by a double-layered net divider (4 cm apart) as described previously (*18*) (fig. S4). Nasal washes were collected every 2 days from all of the animals beginning 2 days p.i. [1 day postexposure (p.e.)] for the detection of virus shedding. Sera were collected from all animals on day 21 p.i. for hemagglutinin inhibition (HI) antibody detection. Respiratory droplet transmission was confirmed when virus was detected in the nasal washes and by seroconversion of the naïve exposed animals at the end of the 3-week observation period.

Virus was detected in all directly infected animals (Fig. 3, F to J). In the exposed groups, virus was not detected in any of the animals exposed to the CK/S1053-inoculated ferrets. However, virus was detected in one ferret exposed to the ferrets that had been inoculated with PG/S1421, SH/1, or SH/2 and in all three ferrets exposed to the ferrets that had been inoculated with AH/1 (Fig. 3J). Because there have been no reports to date of transmission of H7N9 virus among humans, we repeated this respiratory droplet transmission study with AH/1 virus in ferrets and found the results to be reproducible (Fig. 3K). We sequenced the viruses recovered from the inoculated animals on day 6 postinoculation and the viruses recovered from the exposed animals on day 7 p.e. and did not detect any amino acid changes in any of the viruses. Infection of ferrets with the five viruses did not cause marked changes in body temperature (Table 1). The ferrets that were exposed or inoculated with PG/S1421 experienced a 5.8 to 7.6% weight change, and the body-weight loss of ferrets inoculated with the other four viruses was 1.1 to 3.7% (Table 1). Seroconversion occurred in the virus-inoculated animals and in all exposed animals that were virus-positive (Table 1). These results indicate that four of the five H7N9 viruses tested can transmit between ferrets, and one virus, AH/1, transmits highly efficiently between ferrets by respiratory droplet.

Transmission of influenza virus is a polygenic trait. The mutations in HA that confer binding to α-2,6-linked SAs are important for transmission; however, CK/S1053 and AH/1 had similar *HA* genes and bound similarly to the α-2,6-linked SAs, but their transmissibility in ferrets was totally different. PB2 627K is also important for transmission, but SH/1 and SH/2, which both bear PB2 627K, transmitted similarly to PG/S1421, which does not have PB2 627K. Therefore, it is difficult to conclude which amino acid substitution alone makes the virus highly transmissible. However, the amino acid differences between the avian viruses and the AH/1 virus range from 1 to 27 (table S3), suggesting that only a few amino acid changes would be needed to make the avian H7N9 viruses highly transmissible in mammals. Moreover, these changes can occur easily during replication in humans.

In summary, our studies characterized the H7N9 viruses isolated from poultry and humans and demonstrated that these naturally isolated viruses can bind humanlike airway receptors and replicate efficiently in ferrets. Most importantly, one virus isolated from humans is able to transmit efficiently between ferrets by respiratory droplet. The widespread detection of H7N9 viruses from live poultry markets in Shanghai and eight other provinces in a relatively short time period indicates that the viruses transmit efficiently among poultry, especially chickens, and have spread across a wide geographic area in China. Currently, implementation of compulsory control measures in H7N9 virus–positive live poultry markets is preventing further human infections; however, the elimination of the H7N9 virus from nature is a huge and long-term challenge. Its nonpathogenic nature in poultry enables the avian H7N9 virus to replicate silently in avian species and to transmit to humans. Its replication in humans will provide further opportunities for the virus to acquire more mutations and become more virulent and transmissible in the human population.

Reference and Notes

1. S. Tong *et al.*, *Proc. Natl. Acad. Sci. U.S.A.* **109**, 4269–4274 (2012).
2. World Health Organisation, Number of confirmed human cases of avian influenza A(H7N9) reported to WHO, www.who.int/influenza/human_animal_interface/influenza_h7n9/08_ReportWebH7N9Number.pdf (May 2013).
3. See supplementary materials on *Science* Online.
4. J. Shi *et al.*, *Chin. Sci. Bull.* **58**, 1857–1863 (2013).
5. R. Gao *et al.*, *N. Engl. J. Med.* **368**, 1888–1897 (2013).
6. Y. Chen *et al.*, *Lancet* **381**, 1916–1925 (2013).
7. Single-letter abbreviations for the amino acid residues are as follows: A, Ala; C, Cys; D, Asp; E, Glu; F, Phe; G, Gly; H, His; I, Ile; K, Lys; L, Leu; M, Met; N, Asn; P, Pro; Q, Gln; R, Arg; S, Ser; T, Thr; V, Val; W, Trp; and Y, Tyr.
8. E. K. Subbarao, W. London, B. R. Murphy, *J. Virol.* **67**, 1761–1764 (1993).
9. Z. Li *et al.*, *J. Virol.* **79**, 12058–12064 (2005).
10. Y. Gao *et al.*, *PLoS Pathog.* **5**, e1000709 (2009).
11. M. Hatta, P. Gao, P. Halfmann, Y. Kawaoka, *Science* **293**, 1840–1842 (2001).
12. L. Glaser *et al.*, *J. Virol.* **79**, 11533–11536 (2005).
13. M. Matrosovich *et al.*, *J. Virol.* **74**, 8502–8512 (2000).
14. M. Imai *et al.*, *Nature* **486**, 420–428 (2012).
15. S. Herfst *et al.*, *Science* **336**, 1534–1541 (2012).
16. A. Vines *et al.*, *J. Virol.* **72**, 7626–7631 (1998).
17. G. N. Rogers, J. C. Paulson, *Virology* **127**, 361–373 (1983).
18. Y. Zhang *et al.*, *Science* **340**, 1459–1463 (2013).
19. T. Kageyama *et al.*, *Euro Surveill.* **18**, 20453 (2013).
20. *Manual of Diagnostic Tests and Vaccines for Terrestrial Animals* (Office International des Epizooties, Paris, 2011).
21. Q. Li *et al.*, *N. Engl. J. Med.* 130424140638006 (2013).
22. X. Lu *et al.*, *J. Virol.* **73**, 5903–5911 (1999).
23. Y. Li *et al.*, *J. Virol.* **84**, 8389–8397 (2010).
24. Y. Zhang *et al.*, *J. Virol.* **86**, 9666–9674 (2012).
25. A. C. Lowen, S. Mubareka, T. M. Tumpey, A. García-Sastre, P. Palese, *Proc. Natl. Acad. Sci. U.S.A.* **103**, 9988–9992 (2006).
26. C. W. Seibert *et al.*, *J. Virol.* **84**, 11219–11226 (2010).
27. T. M. Tumpey *et al.*, *Science* **315**, 655–659 (2007).

Acknowledgments: We thank S. Watson for editing the manuscript, Y. Shu from the China Centers for Disease Control and Prevention for providing the H7N9 viruses isolated from humans, and the Consortium for Functional Glycomics (Scripps Research Institute, Department of Molecular Biology, La Jolla, CA) for providing the glycans. This work was supported by the Ministry of Agriculture (CARS-42-G08) and by the Ministry of Science and Technology (KJYJ-2013-01-01 and 2012ZX10004214). Virus sequence data from this study were deposited in GenBank with the accession numbers CY146905 to CY147200 and in Global Initiative on Sharing Avian Influenza Data with the accession numbers EPI440678 to 440701 and EIP457614 to 457885.

Supplementary Materials

www.sciencemag.org/cgi/content/full/science.1240532/DC1
Materials and Methods
Supplementary Text
Figs. S1 to S4
Tables S1 to S4
References

15 May 2013; accepted 2 July 2013
Published online 18 July 2013;
10.1126/science.1240532